Conserved *Arabidopsis* ECHIDNA protein mediates *trans*–Golgi-network trafficking and cell elongation

Delphine Gendre[a,1], Jaesung Oh[a,1,2], Yohann Boutté[a], Jacob G. Best[b], Lacey Samuels[b], Robert Nilsson[a], Tomohiro Uemura[c], Alan Marchant[d], Malcolm J. Bennett[e], Markus Grebe[f], and Rishikesh P. Bhalerao[a,3]

[a]Umeå Plant Science Centre, Department of Forest Genetics and Plant Physiology, Swedish University of Agricultural Sciences, S-901 83 Umeå, Sweden; [b]Department of Botany, University of British Columbia, Vancouver, BC, Canada V6T 1Z4; [c]Department of Biological Sciences, University of Tokyo, Bunkyo-ku, Tokyo 113-0033, Japan; [d]School of Biological Sciences, University of Southampton, Southampton SO17 1BJ, United Kingdom; [e]Plant Sciences Division, School of Biosciences, University of Nottingham, Sutton Bonington Campus, Loughborough LE12 5RD, United Kingdom; and [f]Umeå Plant Science Centre, Department of Plant Physiology, Umeå University, S-901 83 Umeå, Sweden

Edited* by Maarten J. Chrispeels, University of California at San Diego, La Jolla, CA, and approved March 28, 2011 (received for review December 10, 2010)

Multiple steps of plant growth and development rely on rapid cell elongation during which secretory and endocytic trafficking via the *trans*-Golgi network (TGN) plays a central role. Here, we identify the ECHIDNA (ECH) protein from *Arabidopsis thaliana* as a TGN-localized component crucial for TGN function. *ECH* partially complements loss of budding yeast *TVP23* function and a *Populus ECH* complements the *Arabidopsis ech* mutant, suggesting functional conservation of the genes. Compared with wild-type, the *Arabidopsis ech* mutant exhibits severely perturbed cell elongation as well as defects in TGN structure and function, manifested by the reduced association between Golgi bodies and TGN as well as mislocalization of several TGN-localized proteins including vacuolar H^+-ATPase subunit a1 (VHA-a1). Strikingly, *ech* is defective in secretory trafficking, whereas endocytosis appears unaffected in the mutant. Some aspects of the *ech* mutant phenotype can be phenocopied by treatment with a specific inhibitor of vacuolar H^+-ATPases, concanamycin A, indicating that mislocalization of VHA-a1 may account for part of the defects in *ech*. Hence, ECH is an evolutionarily conserved component of the TGN with a central role in TGN structure and function.

secretory pathway | dwarf mutant | vacuolar defect

Cell division and anisotropic cell expansion determine the final size and shape of plant organs. Cell expansion poses a mechanistic problem to plant cells, because their plasma membrane is surrounded by a cell wall. Cell elongation requires modulation of cell wall components, involving delivery of cell wall polysaccharides and proteins needed for cell wall remodeling. Additionally, signaling proteins, such as receptors and proteins involved in nutrient and hormonal transport, have to be regulated at the plasma membrane. However, molecular components of vesicle trafficking and protein targeting are only starting to be discovered in plants.

Recently, the *trans*-Golgi network (TGN) has been identified as a key component for plant vesicle trafficking and protein targeting that is required for cell elongation (1, 2). The TGN is a tubular-reticular network derived from the *trans* part of the Golgi, from which it is morphologically and functionally distinct (3, 4). After separation from the Golgi apparatus, the TGN may undergo maturation into early and late compartments (5). The TGN is a highly dynamic structure displaying rapid association/dissociation with Golgi bodies (6, 7), and individual TGNs can undergo reversible homotypic association events (7). The functional importance of the TGN has been highlighted by experimental disruption of vesicle trafficking and cell expansion by perturbing the function of the TGN-localized vacuolar H^+-ATPase (V-ATPase) subunit a1 by using genetical and pharmacological approaches (VHA-a1) (2).

Endocytic and secretory traffic intersect at the TGN in *Arabidopsis* and tobacco, and roles of the TGN in vacuolar sorting as well as secretory targeting have been reported (8, 9). Cargo destined for the plasma membrane or for secretion, e.g., the receptor kinase BRASSINOSTEROID INSENSITIVE1 (BRI1), cell-wall components like xyloglucans, or the secretion reporter-secreted green fluorescent protein (secGFP), transit the TGN on the way to the plasma membrane (7) presumably on TGN-derived mobile secretory vesicles that deliver components to plasma membrane, as shown for tobacco BY-2 cells (10). Additionally TGN receives endocytosed material from the plasma membrane (1, 7, 11), revealing its role in the anterograde late secretory pathway and the retrograde early endosomal (EE) trafficking.

Although several proteins have been localized to the TGN, our knowledge of its structure and molecular function in plants remains limited. Moreover, the secretory and endocytic pathways intersect at the TGN, but how these two trafficking pathways are regulated and how their separation is achieved remains poorly understood. Here, we report that the ECHIDNA (ECH) protein from *Arabidopsis thaliana* is required for cell elongation in *Arabidopsis*. Importantly, we show that ECH is an evolutionary conserved component within *A. thaliana*, hybrid aspen, and budding yeast that is required for correct localization of TGN-resident proteins, TGN integrity, and protein secretion via the TGN.

Results

ECHIDNA Is Required for Cell Elongation in *Arabidopsis*. Plant cells, e.g., root cells (12), frequently undergo several fold increases of their original dimensions during growth and development. To discover components contributing to cell elongation, we investigated publicly available microarray datasets describing gene expression in cell types with rapid expansion, both in *Arabidopsis* and in hybrid aspen (*Populus tremula* × *P. tremuloides)* (13–15). This analysis identified *At1g09330* to be consistently expressed at higher levels in all of the datasets in tissues and cell types undergoing elongation and expansion in both *Arabidopsis* and *Populus* (see *SI Materials and Methods* for details). To address the function of this gene, a T-DNA insertion (SAIL_163_E09) in the homologous *Arabidopsis* sequence (At1g09330) was analyzed. Based on its phenotypic appearance, we named the mutant line *echidna* (*ech*) (Fig. 1*A*). Analysis of the *ech* mutant revealed a severe size reduction of all organs compared with the WT (Fig. 1 *A–D* and Fig. S1*A*). A reduction of epidermal cell length in the root and hypocotyl of *ech* plants by 34% and 57%, respectively

Author contributions: D.G., A.M., M.J.B., M.G., and R.P.B. designed research; D.G., J.O., J.G.B., L.S., R.N., and A.M. performed research; T.U. contributed new reagents/analytic tools; D.G., Y.B., L.S., M.G., and R.P.B. analyzed data; and D.G., M.G., and R.P.B. wrote the paper.

The authors declare no conflict of interest.

*This Direct Submission article had a prearranged editor.

Freely available online through the PNAS open access option.

[1]D.G. and J.O. contributed equally to this work.

[2]Present address: Centre for Plant Integrative Biology, University of Nottingham, Loughborough LE12 5RD, United Kingdom.

[3]To whom correspondence should be addressed. E-mail: rishi.bhalerao@genfys.slu.se.

This article contains supporting information online at www.pnas.org/lookup/suppl/doi:10.1073/pnas.1018371108/-/DCSupplemental.

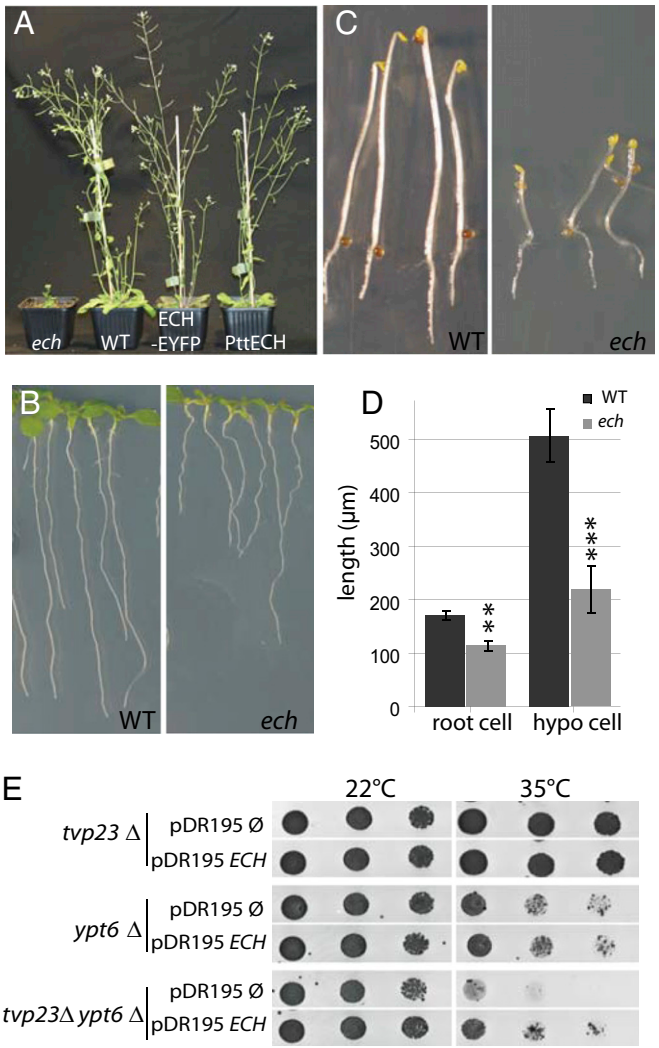

Fig. 1. Characterization of the *Arabidopsis ech* mutant and complementation of yeast *tvp23*Δ by *ECH*. (*A*) Five-week-old *ech* mutant, wild-type Columbia-0 (WT), *ech* rescued by the expression of ECH-EYFP fusion driven by the native ECH promoter (ECH-EYFP), and *ech* rescued by over expression of hybrid aspen PttECH under the 35S-promoter (PttECH). (*B*) Seven-day-old WT and *ech* seedlings. (*C*) Four-day-old etiolated WT and *ech* seedlings. (*D*) Average length of fully elongated epidermal cells from root and dark-grown hypocotyls of WT (black) and *ech* (gray) seedlings. Measurements are an average (±SD) of three biological replicates, each of 50 cells from 12 seedlings. Significant differences determined by Student's *t* test are indicated as $*P < 0.01$ and $**P < 0.001$. (*E*) *tvp23*Δ, *ypt6*Δ and *tvp23*Δ*ypt6*Δ mutant yeast strains transformed with either *ECH* driven from the constitutive *PMA1* promoter or with the empty plasmid. Dilutions of cells were incubated at 22 °C or 35 °C on rich medium plates lacking uracil.

(Fig. 1*D*), correlates with the overall length reduction of those organs (Fig. S1*B*). These data suggest that altered root and etiolated hypocotyl length in *ech* are largely caused by defective cell elongation. Twenty-five percent of plants of a heterozygous segregating population exhibited reduced stature and bushy appearance, suggesting that the phenotype was caused by a single recessive mutation. Southern blot and sequence analysis of genomic DNA from wild-type (WT, Col-0) and homozygous *ech* mutants (Fig. S1*C*, lane 2) confirmed the presence of a single T-DNA insertion in the promoter of *ECH* (Fig. S1*D*). To detect the ECH protein, an affinity-purified antibody was raised against an ECH-derived peptide that detected a single band of 22 kDa on Western blots from WT that was absent in *ech* mutant protein extracts (Fig. S1*E*). These findings are in agreement with a predicted size of ≈20.5 kDa for the 186-aa ECH protein and suggest that *ech* represents a protein-null mutant allele of the *At1g09330* gene. Furthermore, a C-terminal fusion of enhanced yellow fluorescent protein (EYFP) to the ECH protein expressed under control of the *ECH* promoter rescued the *ech* mutant phenotype (Fig. 1*A*), demonstrating the phenotype is caused by an *ECH* defect and that the fluorescent protein fusion is functional.

Evolutionary Conservation of ECH Function. The ECH protein is predicted to have three to four transmembrane domains (Fig. S1*F*) and lacks an N-terminal signal sequence. Sequences homologous to ECH are found in various eukaryotes, suggesting a potential evolutionary conservation of ECH function (Fig. S1*G*). Indeed, the cDNA of ECH homolog from hybrid aspen (PttECH) when driven by the 35S-promoter in the *Arabidopsis ech* mutant background completely restored the mutant phenotype to WT (Fig. 1*A*), highlighting the conservation of ECH function between the annual weed *Arabidopsis* and perennial hybrid aspen trees. Interestingly, ECH also displayed sequence conservation outside the plant kingdom. For example, it shared 34% identity and 53% similarity with the Tlg2p-vesicle protein 23 (Tvp23p) from the budding yeast *Saccharomyces cerevisiae* (16). We therefore investigated whether *ECH* is functionally related to *TVP23*. The yeast *tvp23*Δ mutant does not show perturbed growth, but enhances the phenotype of a mutant defective in the RabGTPase gene *YPT6* ; *tvp23*Δ *ypt6*Δ double mutants are unable to grow at 35 °C but grow at a permissive temperature of 22 °C (ref. 16 and Fig. 1*E*). Importantly, *ECH* expression restored the growth of the *tvp23*Δ *ypt6*Δ double mutant at 35 °C to the same level observed for *ypt6*Δ (Fig. 1*E*, last row), suggesting that ECH can functionally replace yeast TVP23. Thus, aspects of ECH function appear to have been conserved during evolution of plants and budding yeast.

ECH Localizes to the EE/TGN Compartments. We next investigated subcellular localization of ECH in *Arabidopsis* root tip cells by using functional ECH-EYFP (Fig. 1*A*) and the ECH-specific antibody (Fig. S2*A*), whose signals overlap in immunofluorescence microscopy (Fig. S2*B*). ECH-EYFP displayed a punctate pattern in the cytosol and revealed colocalization with TGN compartments labeled by the SNARE SYP41-GFP (Fig. 2*A* and Fig. S2*C*), homologous with yeast Tlg2p (8, 17), VHA-a1-GFP (Fig. 2*A* and Fig. S2*D*) previously shown to colocate at the TGN with SYP41-GFP (1) and SYP61-CFP, closely related to SYP41 (8) (Fig. 2*A* and Fig. S2*E*). Interestingly, a lower degree of colocalization was observed between ECH and RABA2a-YFP (Fig. 2*A* and Fig. S2*F*), which partially colocalizes with the TGN domain labeled by VHA-a1-GFP (18). In contrast, only limited colocalization of ECH signal was observed with late endosomes/multivesicular bodies (MVBs) labeled by the MVB markers (9, 19–21) RABF1-GFP (Fig. 2A and Fig. S2*G*), RABF2b (Fig. 2*A* and Fig. S2*H*), ELP or SYP21 (Fig. 2*A* and Fig. S2 *I* and *J*), and with the Golgi markers EGFP-NAG (22) and *N*-ST-YFP (22, 23) (Fig. 2*A* and Fig. S2 *K* and *L*). In further agreement with ECH localization at early endosomes (EE)/TGN, the endocytic tracer FM4-64 (21) colabeled with ECH-EYFP as rapidly as 3 min after application (Fig. 2*B*). Moreover, upon brefeldin A (BFA) treatment, ECH and VHA-a1 rapidly coaggregated in the core of BFA bodies (Fig. 2*C*) surrounded by *N*-ST-YFP-positive Golgi stacks (Fig. 2*D*) as described for early endosomal and TGN-derived material (22, 24, 25). These results strongly support that ECH largely resides at TGN/EE compartments.

Golgi Structure and TGN-Golgi Association Is Perturbed in *ech*. The TGN localization of ECH prompted us to investigate the ultrastructure of Golgi bodies and TGN in *ech*. No gross malformation of Golgi stacks was observed (Fig. S3) and the number

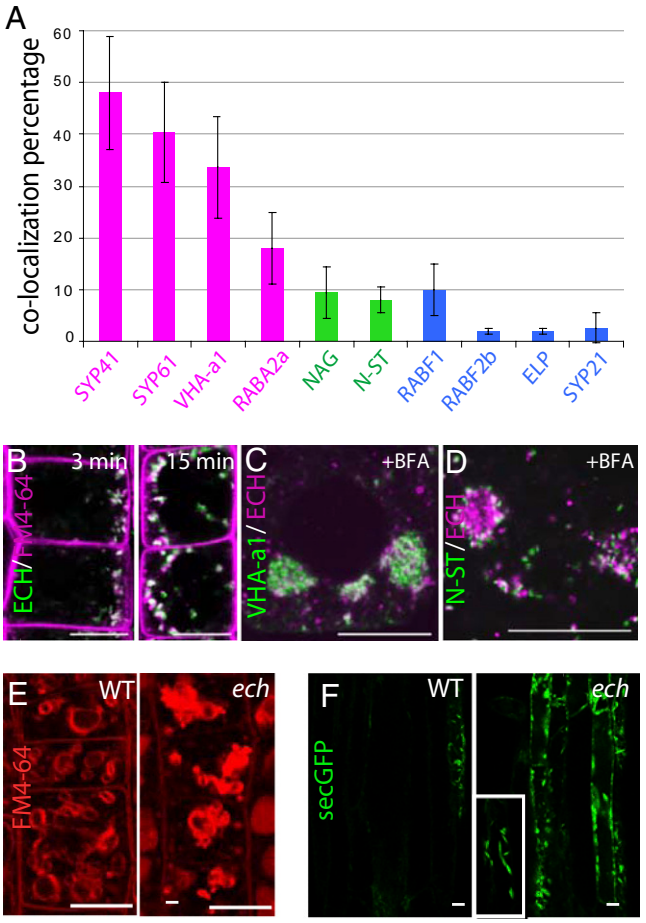

Fig. 2. ECH is a TGN-resident protein and its loss affect secretion. (*A*) Quantitative measurement of colocalization between ECH and markers displayed in Fig. S2. Markers of the TGN (magenta), Golgi apparatus (green), and endosomal and prevacuolar compartments (blue) are indicated by color coding. See *Materials and Methods* for quantification method. (*B*) Colocalization between ECH-EYFP–positive compartments (green) and FM4-64 (magenta), 3 or 15 min after FM4-64 internalization. (*C* and *D*) Colocalization between anti-ECH labeling (magenta) and VHA-a1-GFP (*C*) or *N*-ST-YFP (*D*) fluorescence (green) after 1-h treatment with 50 μM BFA. (*E*) Four hours thirty minutes internalization of FM4-64 in root epidermal cells of WT and *ech*. (*F*) Sec-GFP expression in WT and *ech* backgrounds in elongated epidermal cells. *Inset* is a magnification of sec-GFP in *ech* showing the spindle-shaped of the labeled organelle. (Scale bars: 10 μm.)

of cisternae per Golgi stack was unchanged in the *ech* mutant (4.4 cisternae per stack; $n = 75$ stacks) compared with the WT (4.6 cisternae per stack, $n = 82$ stacks). However, the average width of stack cisternae was significantly decreased in *ech* (685 ± 60 nm, $n = 46$ stacks) compared with WT (1,226 ± 59 nm, $n = 65$; Student's t test, $P < 0.0001$) (Fig. S3). Interestingly, qualitative analysis further revealed 75.4% of the Golgi stacks associated with a TGN in WT, compared with only 34.8% in *ech* ($n = 80$). These results suggest a requirement of ECH function for the length of the Golgi cisternae and the association of TGNs with Golgi stacks.

***ech* Displays Defects in Protein Secretion Rather than Endocytosis.** Our observations prompted us to investigate whether the endocytic or secretory pathways are affected *ech*. Therefore, we analyzed FM4-64 internalization in elongating root epidermal cells of the WT (Fig. S4*A*, *Upper*) and the *ech* mutant (Fig. S4*A*, *Lower*). After 15 min of FM4-64 internalization, large endosomal compartments are stained in both WT and *ech* roots (Fig. S4*A*). Between 1 and 3 h after initial application of FM4-64, MVB-like compartments and provacuoles were observed in both genotypes, whereas the tonoplast was labeled after 4 h 30 min. Incorporation of FM4-64 into vacuolar membranes did not appear to be reduced in the *ech* background compared with WT, but overall vacuolar appearance was altered in *ech* and aggregation of vacuoles was often observed (Fig. 2*E* and Fig. S4*A*). Hence, although internalization from the plasma membrane did not appear to be affected, vacuolar morphology was clearly altered in *ech*. Because the TGN is also involved in secretion, we investigated whether *ech* is defective in the secretory pathway. We used the secGFP reporter that only displays strong accumulation within endomembranes of cells defective in secretion, because secGFP is normally secreted to the cell wall where its fluorescence is quenched due to the acidic apoplastic pH (26). In striking contrast to the WT, secGFP in *ech* was strongly retained inside the cells (Fig. 2*F*), and this signal partially colocalized with the ER marker BIP (27) (Fig. S4*B*), suggesting defective secretion of secGFP in the *ech* mutant. The specificity of the observed secretion defect was further investigated by examining the fate in *ech* roots of other secreted proteins, e.g., the plasma membrane-localized auxin efflux carrier PIN2 and BRI1-YFP. Polar PIN2 localization at the plasma membrane appeared identical in WT and *ech* epidermal and cortical cells (Fig. S4*C*). Similarly, 1 h after induction of heat shock (HS)-inducible *BRI1-YFP*, plasma membranes of WT and *ech* root cells displayed similar BRI1-YFP labeling (Fig. S4*D*). Importantly, the vacuolar transport of proteins e.g., Aleurain-GFP (28, 29) was not affected in *ech* mutant (Fig. S4*E*). Taken together, these results suggested that ECH is required for the route of secretory traffic defined by secGFP but not for all secretory cargos.

Missorting of TGN Proteins to Vacuolar and Cell Plate Compartments. Although most BRI1-YFP correctly localized at the plasma membrane and at the TGN, some BRI1-YFP signal was also observed in vacuoles of the *ech* mutant but not in the WT (Fig. S4*D*, arrows). This mislocalization could imply a defect in BRI1-YFP sorting to the plasma membrane via the TGN (7). Therefore, we investigated the localization of RABA2a-YFP, VHA-a1-GFP, and SYP61-CFP known to reside on partially overlapping domains of the TGN (18). The RABA2a-YFP localization in cell plates and intracellular compartments (Fig. 3*A*) and its rapid colocalization with FM4-64 (Fig. 3*B*) (18) remained unchanged in *ech* (Fig. 3 *C* and *D*). Moreover, after BFA treatment, RABA2a-YFP appeared in the core of BFA-bodies in *ech* similarly to the WT (Fig. S5*A*) (18). However, we additionally observed RABA2a-YFP in amorphous aggregates of various sizes in *ech* meristematic cells (Fig. 3*C*, double arrows), which became more rounded (Fig. 3*G*) and colabeled with FM4-64 (Fig. 3*H*) after long-term internalization in the elongating cells of *ech* mutant, implying their vacuolar nature. Similarly, VHA-a1-GFP and SYP61-CFP displayed partial mislocalization in *ech*. Although VHA-a1-GFP was found in compartments labeled by FM4-64 within 4 min of internalization in both WT (Fig. 3 *I* and *J*) and *ech* (Fig. 3 *K* and *L*), the signal often aggregated in the *ech* mutant (Fig. 3*K*) but still responded to BFA treatment (Fig. S5*A*). In striking contrast to WT (Fig. 3*I*), VHA-a1-GFP also resided at cell plates and vacuolar ring-shaped membranes in *ech* cells (Fig. 3*K*). Tonoplast-like labeling of VHA-a1-GFP persisted in elongated cells (Fig. 3*O*) and colabeled with FM4-64 after 4 h (Fig. 3*P*). Similarly, in *ech,* a part of SYP61-CFP signal localized to the tonoplast of meristematic and elongated cells (Fig. S5*B*) in addition to the punctate-TGN pattern observed in the WT (Fig. S5*B*). Overall these findings suggested missorting of TGN proteins to vacuolar and cell plate compartments in *ech*.

***ech* Is Hypersensitive to Concanamycin A (ConcA) Treatment.** The enlarged VHA-a1-labeled compartments observed in *ech* resembled the abnormal VHA-a1 compartments observed in WT cells treated with ConcA (1), an inhibitor of V-ATPases (30–32).

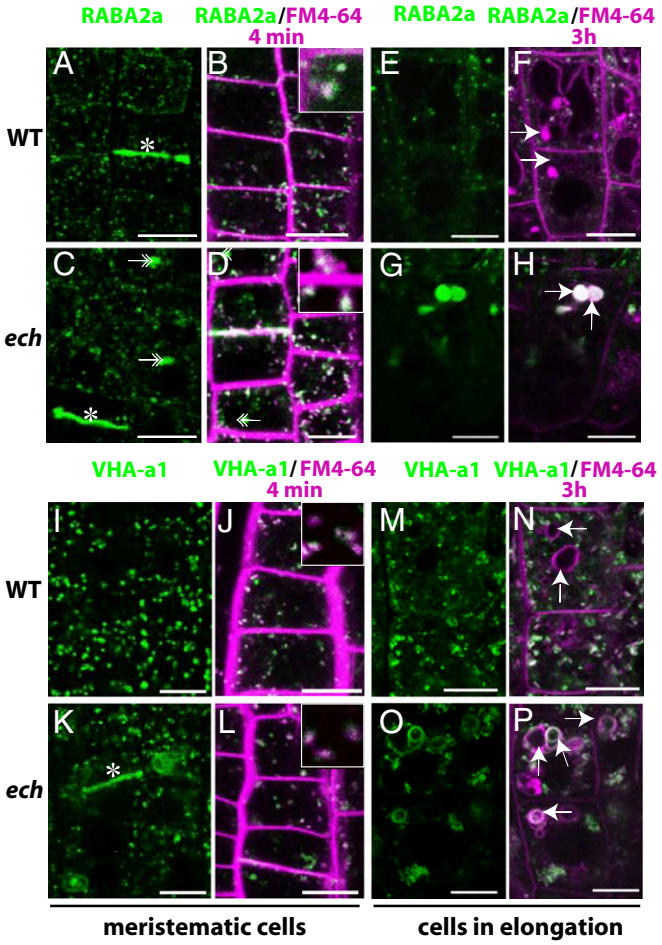

Fig. 3. Mislocalization of the VHA-a1 and RABA2a proteins in *ech*. Confocal images from live root epidermal cells of WT (*A, B, E, F, I, J, M,* and *N*) and *ech* (*C, D, G, H, K, L, O,* and *P*) expressing RABA2a-YFP under control of its own promoter (green) (*A–H*) or VHA-a1-GFP driven by its own promoter (green) (*I–P*). FM4-64 (magenta) internalization was followed after 4 min (*B, D, J,* and *L* and respective insets magnifying of 25×) and 3 h (*F, H, N,* and *P*). Cells chosen are meristematic (*A–D* and *I–L*) or in the elongation zone (*E–H* and *M–P*). Asterisks (*) highlight cell-plate staining and arrows indicate vacuoles. (Scale bars: 10 μm.)

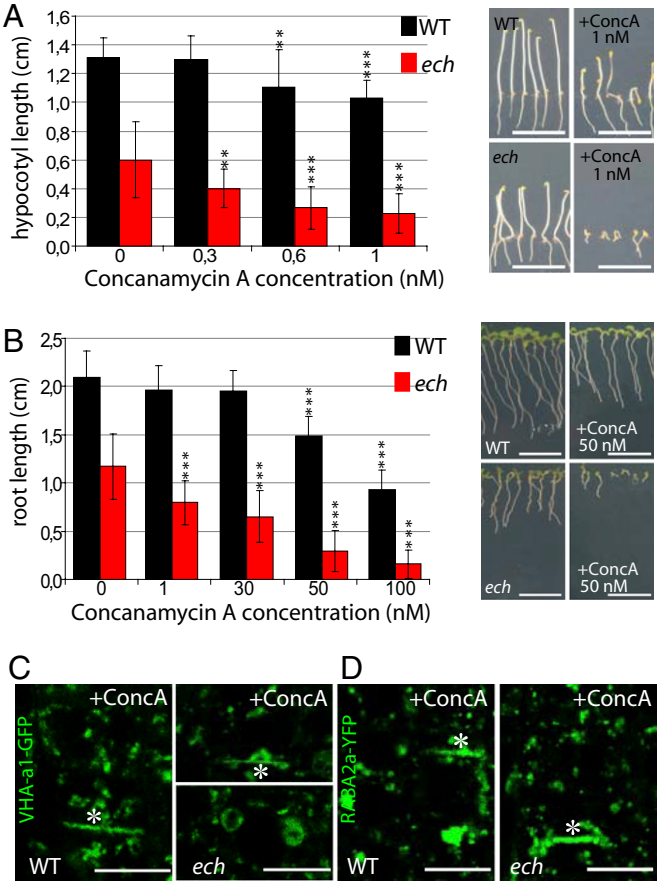

Fig. 4. Concanamycin A treatment phenocopies *ech* mutant phenotypes and *ech* is hypersensitive to ConcA. The effect of ConcA on etiolated hypocotyl (*A*) and root (*B*) lengths of WT (black) and *ech* (red) grown on MS/2 medium supplemented with indicated ConcA concentrations. Measurement from three independent experiments (means ± SD) of 20 seedlings each. *C* and *D* show VHA-a1-GFP (*C*) and RABA2a-YFP (*D*) fluorescence in root epidermal cells of WT (*Left*) and *ech* (*Right*) treated for 1 h with 10 μM ConcA. Note cell plate labeling (*). (Scale bars: 10 μm.)

In agreement with previous work (33), ConcA treatment reduced etiolated hypocotyl (Fig. 4*A*) and root (Fig. 4*B*) length in both WT and *ech* seedlings. However, elongation of both organs in *ech* was hypersensitive to ConcA compared with the WT (Fig. 4 *A* and *B*), Thus, the *ech* mutant defects resemble those caused by the pharmacological inhibition of VHA-a1 by ConcA in the wild type.

Concanamycin A Phenocopies TGN Marker Mislocalization Observed in *ech*. We subsequently investigated the appearance of VHA-a1-GFP– and RABA2a-YFP–labeled compartments after ConcA treatment. As reported (1), VHA-a1-GFP–labeled compartments in WT appeared aggregated after treatment with 10 μM ConcA for 1 h (Fig. 4*C*). Intriguingly, an additional mislocalization of VHA-a1-GFP to cell plates was also observed in WT cells treated with ConcA (Fig. 4*C*, star), as seen in untreated *ech* cells (Fig. 3*K*). Similarly, RABA2a-YFP–labeled compartments displayed aggregation in WT after ConcA treatment (Fig. 4*D*), strongly resembling its distribution in untreated *ech* cells (Fig. 3*C*).

Discussion

ECHIDNA Is Necessary for Cell Elongation. In this study, we identify ECH as an evolutionarily conserved, unique plant protein that localizes to the TGN and plays an important role in its function. Our analyses of the *Arabidopsis ech* mutant revealed that ECH mediates cell elongation in root and shoot epidermal cells.

ECH Localizes to TGN Domain Defined by VHA-a1/SYP41/SYP61 and Is Required for Protein Secretion. The strong colocalization of ECH with the TGN markers SYP41, SYP61, and VHA-a1 suggest that they reside on a common subdomain of the TGN. Furthermore, rapid colabeling of ECH-EYFP with an endocytic tracer is in agreement with the proposed EE function of the TGN (1). However, ECH is not required for the immediate internalization step of endocytic trafficking because FM4-64 internalization remained unperturbed in *ech*. Rather, accumulation of secGFP inside *ech*-mutant cells suggests a function of ECH in the secretory pathway. Given that ECH localizes to the TGN, it may seem surprising that some secGFP was found in the ER. However, the most likely explanation for this observation is that this is a secondary effect of the altered Golgi and/or Golgi-TGN association in *ech* mutants, as discussed below. It may initially appear surprising that accumulation of BRI1 and PIN2 at the plasma membrane did not seem to be perturbed in *ech*, although BRI1 is exocytosed via the TGN, like secGFP (7). However, accumulation of BRI1 in vacuolar structures may be consistent with a diversion of some BRI1 protein into the vacuolar targeting pathway. ECH may therefore be required for keeping the appropriate balance

between secretory trafficking and vacuolar targeting of a subset of proteins.

ECH Is Required for Proper Localization of TGN Resident Proteins. A major defect in the *ech* mutant is the mislocalization of the proteins VHA-a1, SYP61, RabA2a, and BRI1, which localize to and traffic via the TGN/EE (7, 34). Hence, ECH function appears essential for correct localization of these proteins at the TGN and an important question is what leads to their mislocalization in the *ech* mutant. This mislocalization may not be primarily due to structural defects, because ultrastructural analysis of *ech* mutant cells did not reveal structural defects in the TGN, but rather a reduced association of TGN with Golgi stacks. This reduced association could potentially reflect an alteration of the dynamic interaction between the TGN and Golgi apparatus. As shown recently, individual TGN compartments dynamically interact with Golgi stacks (7). Importantly, not all TGN compartments are able to interact with each other, suggesting potential regulation of these events. Hence, a possible function of ECH could be to prevent SYP61-, VHA-a1-, RABA2a-, and BRI1-positive compartments from interacting with other TGN compartments from which proteins might be targeted to the vacuoles.

Inappropriate Trafficking of VHA-a1 May Explain Aspects of the *ech* Phenotype. Cell elongation relies on the secretory system to deliver cell wall components, together with a variety of proteins and enzymes involved in cell wall remodeling, to the cell periphery. Given the secGFP secretion defects observed in *ech*, it is not surprising that the mutant displays cell elongation defects, particularly because secGFP appears to use a similar secretory pathway to pectins in BY-2 cells (10).

Several lines of evidence reveal that abnormalities in *ech* may arise from the mislocalization of key TGN components including VHA-a1. VHA-a1 has an integral role in both TGN function and cell elongation, with several studies showing that V-ATPases are crucial for cell expansion in *Arabidopsis* (2, 33, 35–37). Among the three isoforms of the VHA subunit a in *Arabidopsis*, VHA-a1 is the only nontonoplastic one and its specific inhibition is sufficient to inhibit cell expansion (2).

Several aspects of the *ech* mutant phenotype could be phenocopied in WT by ConcA application. Treatment with ConcA causes growth inhibition (ref. 33 and this work), mislocalization of VHA-a1-GFP (1), and defective protein secretion (7). All these aberrations are also observed in *ech* in the absence of ConcA treatment. Furthermore, BRI1 also mislocalizes to vacuoles after ConcA treatment (38). It is therefore likely that such defects in *ech* are related to VHA-a1 mislocalization. This hypothesis is further supported by the hypersensitivity of *ech* to ConcA treatment. Such hypersensitivity could be caused by partial VHA-a1 mislocalization resulting in less functional V-ATPase being present on the endomembrane compartment in *ech* compared with the WT. Another consequence of less VHA-a1 at the TGN might be the reduced association of TGN with Golgi in *ech*. The TGN has been suggested to be derived from Golgi and electron tomographic analyses, suggesting that the TGN is sloughed off from Golgi stacks (5). Moreover, inhibition of VHA-a1 coincides with aberrant Golgi structure and loss of TGN identity (1, 7).

Our data suggest that perturbed trafficking of VHA-a1 is the most straightforward explanation of the defects observed in *ech*. Recent research in mammals, yeast, and plants extended the role of V-ATPase implicated primarily in energizing membranes in eukaryotic cells by proton extrusion (39), V-ATPases are now increasingly known to be involved in vesicle formation, membrane trafficking, and membrane fusion (40, 41). For example, ARNO/ARF6 is recruited onto membranes via its interaction with the Vo sector subunit a2, in a luminal–pH-dependant manner, before recruitment of coatomer proteins essential for vesicle formation (42), indicating a role for V-ATPases in vesicular trafficking. Therefore, targeting and vesicular trafficking of V-ATPases to specific membranes is an important regulatory mechanism for acidification and vesicular trafficking per se; it may then not be surprising that mislocalization of VHA-a1 in *ech* leads to defects in trafficking.

ECH Localization and Function May Be Conserved Among Eukaryotes. Proteins similar to ECH are found in most eukaryotic genomes, suggesting that its conservation reflects a fundamental cellular function. However, the exact molecular nature of this function remains unknown. The loss of yeast *ECH* ortholog *TVP23* does not lead to an easily observable phenotype, but the suppression of the *ech* mutant phenotype by *PttECH*, and the suppression of *tvp23*Δ/*ypt6*Δ yeast double mutant growth defects by *ECH* show that ECH function is at least partially conserved among perennial trees, annual plants, and yeast.

Importantly, it has been shown that the yeast ortholog of VHA-a1 (STV1p), continuously cycles between the PVC and the late Golgi but is concentrated back at the late Golgi at steady state (43). Interestingly, like in the *ech* mutant, many small unfused vacuoles are observed in yeast when STV1p localization is altered, e.g., by ectopic expression at the vacuole (44), or when *STV1* is mutated (45). These observations would suggest that mechanisms must exist that are crucial to maintain the correct steady-state localization of VHA-a1 and STV1p in plants and yeast, respectively, and that ECH may play a key role in maintaining correct localization of VHA-a1 in plants. The factors involved in maintaining STV1p localization remain unknown in yeast and whether TVP23 could play a role in this process remains to be investigated.

Further clues toward ECH function can be derived from work on TVP23 in yeast. The *tvp23*Δ mutation enhances both the *ypt6*Δ (16) and the *vti1-2* (46) yeast mutant phenotypes. The Ypt6p and Vti1p proteins play a role in transport of carboxypeptidase A and alkaline phosphatase transport to the vacuole, but no conclusive effect was recorded in *tvp23*Δ concerning their routing (16, 46). Similarly, no defect of aleurain transport to the vacuole was observed in *ech*. TVP23 has also been shown to have a role in the retrograde pathway between TGN and Golgi in budding yeast (46), which might provide an explanation for the smaller Golgi stacks found in *ech* mutant. A defect in the retrograde pathway could also well explain the reduced TGN-Golgi association observed in the *ech* mutant that, in turn, could lead to the defect in the secretion of secGFP.

Taken together, we identified ECH as a unique component of the plant TGN with a conserved role in poplar, *Arabidopsis*, and yeast. Although the TGN is clearly an important cellular compartment, several aspects of its structure and function remain largely unexplored in plants. Identification of ECH thus represents an important step toward understanding of TGN structure and function. Further investigation of ECH and other proteins that it interacts with should provide significant insight into the diverse roles of TGN function in plant growth and development.

Materials and Methods

Plant Material. The *ech* T-DNA insertion mutant line (SAIL_163_E09, Col0, Basta^R) was obtained from the SALK Institute. See *SI Materials and Methods* for details.

Bioinformatic Analysis for Selection of *ECHIDNA* for Functional Analysis. See *SI Materials and Methods* for details.

Root, Hypocotyl, and Cell Lengths Measurement. See *SI Materials and Methods* for details.

Plasmid Construction and Plant Transformation. See *SI Materials and Methods* for details.

Antibody Production. Amino-terminal 20-aa sequences (MDPNNQIQAP VENYANPRTC) were used to raise a rabbit antiserum (AgriSera). The serum was purified by immunoaffinity using the peptide as bait fixed on the column.

Confocal Laser-Scanning Microscopy, Immunostaining, FM4-64 Staining, and Inhibitor Treatments. See *SI Materials and Methods* for details.

Quantitative Analysis of Colocalization. See *SI Materials and Methods* for details.

Yeast Complementation. See *SI Materials and Methods* for details.

ACKNOWLEDGMENTS. We thank I. Moore, K. Schumacher, N. Geldner, K. Palme, K. Yoda and T. Ueda for sharing published research materials that were important to this study; N. Raikhel for providing materials and thoughtful comments; E. Johnson for critically reading the manuscript; and A. Sjödin for help with quantification of colocalization. This work was supported by a grant from European Union Project ENERGYPOPLAR, Funcfiber and Formas (to R.P.B.) and a Discovery Grant to L.S. from the Canadian Natural Sciences and Engineering Research Council.

1. Dettmer J, Hong-Hermesdorf A, Stierhof YD, Schumacher K (2006) Vacuolar H+-ATPase activity is required for endocytic and secretory trafficking in Arabidopsis. *Plant Cell* 18:715–730.
2. Brüx A, et al. (2008) Reduced V-ATPase activity in the trans-Golgi network causes oxylipin-dependent hypocotyl growth Inhibition in Arabidopsis. *Plant Cell* 20: 1088–1100.
3. Moore PJ, Swords KM, Lynch MA, Staehelin LA (1991) Spatial organization of the assembly pathways of glycoproteins and complex polysaccharides in the Golgi apparatus of plants. *J Cell Biol* 112:589–602.
4. Zhang GF, Staehelin LA (1992) Functional compartmentation of the Golgi apparatus of plant cells: Immunocytochemical analysis of high-pressure frozen- and freeze-substituted sycamore maple suspension culture cells. *Plant Physiol* 99:1070–1083.
5. Staehelin LA, Kang BH (2008) Nanoscale architecture of endoplasmic reticulum export sites and of Golgi membranes as determined by electron tomography. *Plant Physiol* 147:1454–1468.
6. Crowell EF, et al. (2009) Pausing of Golgi bodies on microtubules regulates secretion of cellulose synthase complexes in Arabidopsis. *Plant Cell* 21:1141–1154.
7. Viotti C, et al. (2010) Endocytic and secretory traffic in Arabidopsis merge in the trans-Golgi network/early endosome, an independent and highly dynamic organelle. *Plant Cell* 22:1344–1357.
8. Bassham DC, Sanderfoot AA, Kovaleva V, Zheng H, Raikhel NV (2000) AtVPS45 complex formation at the trans-Golgi network. *Mol Biol Cell* 11:2251–2265.
9. Sanderfoot AA, et al. (1998) A putative vacuolar cargo receptor partially colocalizes with AtPEP12p on a prevacuolar compartment in Arabidopsis roots. *Proc Natl Acad Sci USA* 95:9920–9925.
10. Toyooka K, et al. (2009) A mobile secretory vesicle cluster involved in mass transport from the Golgi to the plant cell exterior. *Plant Cell* 21:1212–1229.
11. Galway ME, Rennie PJ, Fowke LC (1993) Ultrastructure of the endocytotic pathway in glutaraldehyde-fixed and high-pressure frozen/freeze-substituted protoplasts of white spruce (Picea glauca). *J Cell Sci* 106:847–858.
12. Swarup R, et al. (2007) Ethylene upregulates auxin biosynthesis in Arabidopsis seedlings to enhance inhibition of root cell elongation. *Plant Cell* 19:2186–2196.
13. Zimmermann P, Hirsch-Hoffmann M, Hennig L, Gruissem W (2004) GENEVESTIGATOR. Arabidopsis microarray database and analysis toolbox. *Plant Physiol* 136:2621–2632.
14. De Rybel B, et al. (2010) A novel aux/IAA28 signaling cascade activates GATA23-dependent specification of lateral root founder cell identity. *Curr Biol* 20:1697–1706.
15. Hertzberg M, et al. (2001) A transcriptional roadmap to wood formation. *Proc Natl Acad Sci USA* 98:14732–14737.
16. Inadome H, Noda Y, Kamimura Y, Adachi H, Yoda K (2007) Tvp38, Tvp23, Tvp18 and Tvp15: novel membrane proteins in the Tlg2-containing Golgi/endosome compartments of Saccharomyces cerevisiae. *Exp Cell Res* 313:688–697.
17. Sanderfoot AA, Assaad FF, Raikhel NV (2000) The Arabidopsis genome. An abundance of soluble N-ethylmaleimide-sensitive factor adaptor protein receptors. *Plant Physiol* 124:1558–1569.
18. Chow CM, Neto H, Foucart C, Moore I (2008) Rab-A2 and Rab-A3 GTPases define a trans-golgi endosomal membrane domain in Arabidopsis that contributes substantially to the cell plate. *Plant Cell* 20:101–123.
19. Ahmed SU, Bar-Peled M, Raikhel NV (1997) Cloning and subcellular location of an Arabidopsis receptor-like protein that shares common features with protein-sorting receptors of eukaryotic cells. *Plant Physiol* 114:325–336.
20. Kotzer AM, et al. (2004) AtRabF2b (Ara7) acts on the vacuolar trafficking pathway in tobacco leaf epidermal cells. *J Cell Sci* 117(Pt 26):6377–6389.
21. Ueda T, Yamaguchi M, Uchimiya H, Nakano A (2001) Ara6, a plant-unique novel type Rab GTPase, functions in the endocytic pathway of Arabidopsis thaliana. *Embo J* 20: 4730–4741.
22. Grebe M, et al. (2003) Arabidopsis sterol endocytosis involves actin-mediated trafficking via ARA6-positive early endosomes. *Curr Biol* 13:1378–1387.
23. Batoko H, Zheng HQ, Hawes C, Moore I (2000) A rab1 GTPase is required for transport between the endoplasmic reticulum and golgi apparatus and for normal golgi movement in plants. *Plant Cell* 12:2201–2218.
24. Geldner N, et al. (2003) The Arabidopsis GNOM ARF-GEF mediates endosomal recycling, auxin transport, and auxin-dependent plant growth. *Cell* 112:219–230.
25. Lam SK, et al. (2009) BFA-induced compartments from the Golgi apparatus and trans-Golgi network/early endosome are distinct in plant cells. *Plant J* 60:865–881.
26. Teh OK, Moore I (2007) An ARF-GEF acting at the Golgi and in selective endocytosis in polarized plant cells. *Nature* 448:493–496.
27. Tamura K, Yamada K, Shimada T, Hara-Nishimura I (2004) Endoplasmic reticulum-resident proteins are constitutively transported to vacuoles for degradation. *Plant J* 39:393–402.
28. Di Sansebastiano GP, Paris N, Marc-Martin S, Neuhaus JM (2001) Regeneration of a lytic central vacuole and of neutral peripheral vacuoles can be visualized by green fluorescent proteins targeted to either type of vacuoles. *Plant Physiol* 126:78–86.
29. Fluckiger R, et al. (2003) Vacuolar system distribution in Arabidopsis tissues, visualized using GFP fusion proteins. *J Exp Bot* 54:1577–1584.
30. Huss M, et al. (2002) Concanamycin A, the specific inhibitor of V-ATPases, binds to the V(o) subunit c. *J Biol Chem* 277:40544–40548.
31. Wang Y, Inoue T, Forgac M (2005) Subunit a of the yeast V-ATPase participates in binding of bafilomycin. *J Biol Chem* 280:40481–40488.
32. Bowman EJ, Bowman BJ (2005) V-ATPases as drug targets. *J Bioenerg Biomembr* 37: 431–435.
33. von der Fecht-Bartenbach J, et al. (2007) Function of the anion transporter AtCLC-d in the trans-Golgi network. *Plant J* 50:466–474.
34. Geldner N, Hyman DL, Wang X, Schumacher K, Chory J (2007) Endosomal signaling of plant steroid receptor kinase BRI1. *Genes Dev* 21:1598–1602.
35. Dettmer J, et al. (2005) Essential role of the V-ATPase in male gametophyte development. *Plant J* 41:117–124.
36. Padmanaban S, Lin X, Perera I, Kawamura Y, Sze H (2004) Differential expression of vacuolar H+-ATPase subunit c genes in tissues active in membrane trafficking and their roles in plant growth as revealed by RNAi. *Plant Physiol* 134:1514–1526.
37. Schumacher K, et al. (1999) The Arabidopsis det3 mutant reveals a central role for the vacuolar H(+)-ATPase in plant growth and development. *Genes Dev* 13:3259–3270.
38. Kleine-Vehn J, et al. (2008) Differential degradation of PIN2 auxin efflux carrier by retromer-dependent vacuolar targeting. *Proc Natl Acad Sci USA* 105:17812–17817.
39. Saroussi S, Nelson N (2009) The little we know on the structure and machinery of V-ATPase. *J Exp Biol* 212(Pt 11):1604–1610.
40. Marshansky V, Futai M (2008) The V-type H+-ATPase in vesicular trafficking: targeting, regulation and function. *Curr Opin Cell Biol* 20:415–426.
41. Wada Y, Sun-Wada GH, Tabata H, Kawamura N (2008) Vacuolar-type proton ATPase as regulator of membrane dynamics in multicellular organisms. *J Bioenerg Biomembr* 40:53–57.
42. Hurtado-Lorenzo A, et al. (2006) V-ATPase interacts with ARNO and Arf6 in early endosomes and regulates the protein degradative pathway. *Nat Cell Biol* 8:124–136.
43. Kawasaki-Nishi S, Bowers K, Nishi T, Forgac M, Stevens TH (2001) The amino-terminal domain of the vacuolar proton-translocating ATPase a subunit controls targeting and in vivo dissociation, and the carboxyl-terminal domain affects coupling of proton transport and ATP hydrolysis. *J Biol Chem* 276:47411–47420.
44. Kawasaki-Nishi S, Nishi T, Forgac M (2001) Yeast V-ATPase complexes containing different isoforms of the 100-kDa a-subunit differ in coupling efficiency and in vivo dissociation. *J Biol Chem* 276:17941–17948.
45. Perzov N, Padler-Karavani V, Nelson H, Nelson N (2002) Characterization of yeast V-ATPase mutants lacking Vph1p or Stv1p and the effect on endocytosis. *J Exp Biol* 205 (Pt 9):1209–1219.
46. Stein IS, Gottfried A, Zimmermann J, Fischer von Mollard G (2009) TVP23 interacts genetically with the yeast SNARE VTI1 and functions in retrograde transport from the early endosome to the late Golgi. *Biochem J* 419:229–236.